Electrostatic Potential Surface Analysis of the Transition State for AMP Nucleosidase and for Formycin 5′-Phosphate, a Transition-State Inhibitor†

Joel I. Ehrlich and Vern L. Schramm*

Department of Biochemistry, Albert Einstein College of Medicine, 1300 Morris Park Avenue, Bronx, New York 10461

Received March 7, 1994; Revised Manuscript Received April 29, 1994®

ABSTRACT: AMP nucleosidase hydrolyzes the N-glycosidic bond of AMP to yield adenine and ribose 5-phosphate. Kinetic isotope effects have been used to establish an experimentally based transition-state structure for the native enzyme and a V_{max} mutant [Mentch, F., Parkin, D. W., & Schramm, V. L. (1987) *Biochemistry 26*, 921–930; Parkin, D. W., Mentch, F., Banks, G. A., Horenstein, B. A., & Schramm, V. L. (1991) *Biochemistry 30*, 4586–4594]. The transition states are characterized by weak reaction coordinate bonds to C1′ and substantial carbocation character in the ribose ring. The N9–C1′ bond to the leaving group is nearly broken and the adenine ring is protonated at the transition state. Formycin 5′-phosphate and other purine nucleoside 5′-phosphate analogues with *syn*-glycosyl torsion angles bind better than substrate, supporting a *syn* configuration in the enzyme–substrate complex and presumably in the transition state [Giranda, V. L., Berman, H. M., & Schramm, V. L. (1988) *Biochemistry 27*, 5813–5818]. Access to a geometric model of the transition state permits the analysis of its molecular electrostatic potential surface as enforced by the enzyme. Comparison of the molecular electrostatic potential surfaces for AMP, formycin 5′-phosphate, and the transition state reveals a striking similarity in the surface charges of formycin 5′-phosphate and the transition state. The enzyme-stabilized transition state for AMP hydrolysis is characterized by new positive electrostatic potential in the adenine ring as a result of protonation by the enzyme. This is closely matched by the protonated pyrazole ring of formycin 5′-phosphate. The molecular electrostatic potential surfaces of formycin 5′-phosphate and the transition state for AMP are similar and are likely to be a factor in the K_m/K_i value of $>10^3$ for formycin 5′-phosphate as a transition-state inhibitor of AMP nucleosidase.

The nature of transition states for enzymatic reactions is critical for the detailed understanding of their chemical mechanisms. Transition-state theory posits that enzymes achieve catalysis though stabilization of these high-energy, short-lived structures, binding them with high specificity and more tightly than their substrates by a factor equivalent to the enzymatic rate enhancement (Wolfenden, 1979). Comparison of the acid-catalyzed and enzymatic solvolysis of the N-glycosidic bond of AMP indicates a rate acceleration of 6×10^{12} (DeWolf et al., 1986). Compounds which are postulated to be mimics of the transition state have also been used as inhibitors to evaluate mechanistic hypotheses [e.g., Morrison and Walsh (1988)]. Knowledge of transition-state structure permits inhibitor design by incorporating geometric and electrostatic features of the transition state into stable analogues (Horenstein & Schramm, 1993a,b; Boutellier et al., 1994).

Kinetic isotope effects for the reaction catalyzed by AMP nucleosidase report on the bond orders of participating chemical linkages at the energy maximum. Subsequent computational bond-energy/bond-order vibrational analyses (BEBOVIB) and applications of Pauling's rule (relating bond orders to bond length) have resulted in experimental determinations of the molecular geometry at the transition state for this and related enzymes (Sims & Lewis, 1984; Mentch et al., 1987; Markham et al., 1987; Parkin et al., 1991; Horenstein et al., 1991). Recently, this laboratory has applied semiempirical and ab initio molecular orbital calculations to these experimentally devised structures to characterize the molecular electrostatic potential surfaces of transition states and inhibitors (Horenstein & Schramm, 1993a,b; Kline & Schramm, 1994). This approach provides information for the charges and electronic distribution as substrate is converted to the transition state. These charges have been proposed to be the sources of transition-state-specific interactions with charged groups on the enzyme (Warshel et al., 1989; Warshel, 1991). Even in the absence of protein structural information, electrostatic potential surfaces of the transition state indicate the types of electrostatic interactions the enzyme might use to stabilize the transition state and thereby achieve catalysis. Transition-state molecular electrostatic potentials are expected to be useful in docking studies within the X-ray crystal structures of proteins, as it is not possible to cocrystalize enzymes with authentic transition-state structures. Finally, these analyses provide a geometric and electrostatic blueprint for use in rational design of optimal transition-state inhibitors. Application of these methods to nucleoside hydrolase has resulted in a family of transition-state inhibitors (Horenstein & Schramm, 1993b; Boutellier et al., 1994).

This report describes molecular electrostatic potential calculations on the substrate, transition state, and an inhibitor (formycin 5′-PO_4) of AMP nucleosidases from *Azotobacter vinelandii*. The enzyme catalyzes the reversible hydrolysis of adenosine monophosphate (eq 1) and is presumed to play a

$$\text{AMP} + \text{H}_2\text{O} \overset{\text{MgATP}}{\rightleftarrows} \text{adenine} + \text{ribose 5-PO}_4 \qquad (1)$$

role in the regulation of the adenylate pool in this organism (Schramm & Leung, 1973). MgATP is a V_{max} allosteric

† This work was supported by Research Grants GM21083 and GM41916 from the National Institutes of Health. J.I.E. is an NSF Predoctoral Fellow.

* Corresponding author [telephone (718) 430-2813; FAX (718) 892-0703; email vern@aecom.yu.edu].

® Abstract published in *Advance ACS Abstracts,* July 1, 1994.

0006-2960/94/0433-8890$04.50/0

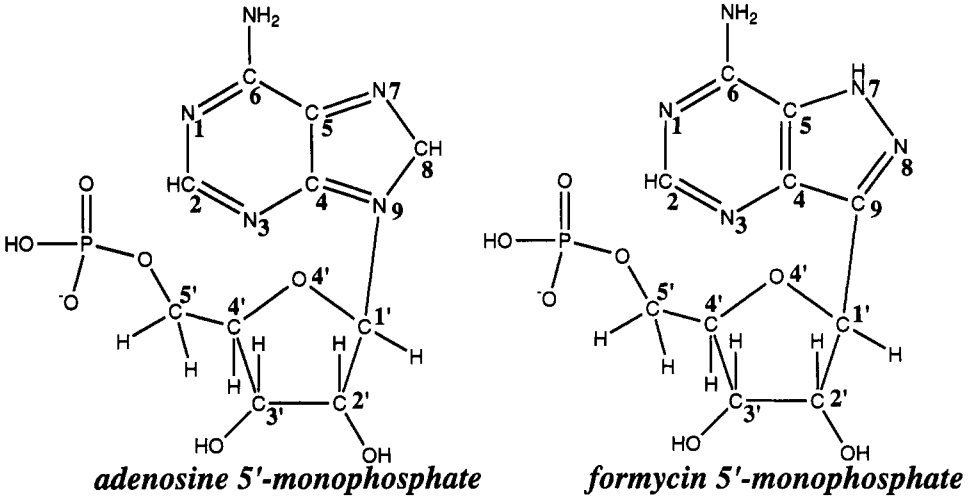

FIGURE 1: Atomic numbering for adenosine 5′-PO_4 (AMP) and formycin 5′-PO_4. For purposes of comparison, the same numbering system is used for both structures. The IUPAC numbering of the fused pyrazolopyrimidine ring system assigns highest priority to the pyrazole ring system [e.g., Suhadolnik (1979)], where the atoms corresponding to N7, C8, and N9 in AMP are N1, N2, and C3, respectively.

activator, resulting in a 200–1000-fold increase in turnover number, depending on substrate concentration (Schramm, 1974). Kinetic isotope effects and bond-energy/bond-order vibrational analyses have previously been employed to describe the transition-state geometries for acid-catalyzed solvolysis and for the enzyme with and without activation by MgATP. Distinct families of kinetic isotope effects are observed for acid-catalyzed solvolysis and for enzyme in the presence and absence of MgATP, suggesting that the transition states are also different (Parkin et al., 1984; Parkin & Schramm, 1984). Their structures provide insight into the mechanism of enzyme-catalyzed solvolysis and of allosteric activation, even though the structure of the protein is unknown (Parkin & Schramm, 1987; Mentch et al., 1987). The transition states of a V_{max} mutant enzyme of AMP nucleosidase have also been determined in the presence and absence of allosteric activation (Parkin et al., 1991). The reaction for the AMP nucleosidases thus far examined is concerted, but the observed enzymatic isotope effects do not fit neatly to an S_N1 or S_N2 model. The ribose C1′ develops a significant degree of sp^2 hybridization at the transition state, but a bond order of up to 0.21 remains between C1′ and N9 of the adenine leaving group (which is protonated at N7). The rehybridization at C1′ is delocalized by resonance with an O4′ oxycarbonium, and β-secondary ^{2}H2′ isotope effects support hyperconjugation with this proton as well. The sp^2 geometry at C1′ forces the ribose ring pucker to be 3′-exo, and substrate and inhibitor specificity suggests that the purine ring is in the *syn* configuration around the glycosyl bond (DeWolf, 1979; Giranda et al., 1988). These data have been incorporated into the geometric model of the transition state for AMP nucleosidase. The transition-state structure described here is derived from experimental kinetic isotope effects, a method distinct from the often used ab initio determination of putative transition states by locating energy maxima along the reaction coordinate with molecular orbital calculations (Gouverneur et al., 1993)

Formycin 5′-phosphate (Figure 1) binds 1200–2600 times tighter than substrate to AMP nucleosidases from various sources. This analogue has a *syn* conformation, a C–C glycosidic bond, and a protonated aglycon in the position which corresponds to N7 of AMP, which is also postulated to be protonated at the transition state (Mentch et al., 1987). These features suggest that formycin 5′-PO_4 may be both a geometric and charge mimic of the transition state. The purpose of this study is to compare the molecular electrostatic potential surfaces of substrate, transition state, and proposed transition-state inhibitor. A geometric model of the transition state, based on kinetic isotope effects (Figure 2), forms the basis for this analysis.

METHODS

Molecular Orbital Calculations, Molecular Electrostatic Potential Calculations, and Visualization. The geometries of AMP, formycin 5′-PO_4, and the transition states were preminimized within the structure constraints described below, using the semiempirical AM1 basis set in the MOPAC 6.0 program package (Merz & Besler, 1990). All bond angles not constrained in the original starting structures were then fixed. The ab initio STO-3G basis set was used to calculate the wave functions for the preminimized systems by the DIRECT self-consistent field algorithm of Gaussian 92 (Frisch et al., 1992). The electron densities and electrostatic potential surfaces of the systems were determined from the wave functions using the CUBE option of Gaussian 92. Results were visualized with the AVS Chemistry Viewer package (Advanced Visual Systems Inc. and Molecular Simulations Inc.). Color maps for potential surfaces were chosen to yield maximum contrast for a system of a given net charge. Maps covering the same charge range but differing in the absolute charge values represented by a color were used separately for systems of −1, 0, and +1 net charge. Representative calculations were also performed using the 6-31G basis set. The relative locations of partial positive and negative charge were found to be independent of the choice of basis set.

Initial Geometries. It was necessary to specify the geometries of the input structures and constrain them such that the final results would retain features known to be involved in the enzymatic interactions. For example, constraint-free structural minimization of AMP, reactant N7-protonated AMP, and formycin all yield different glycosyl torsion angles and phosphate configurations. However, it is likely that the 5′-phosphoryl arm from bound AMP, N7-protonated AMP, the transition state of AMP, and formycin 5′-PO_4 interacts with the same charged locus on the enzyme. Constraints were applied to prevent the phosphoryl from interacting with the partial positive charge at N7 in formycin 5′-PO_4 and at the transition state. Glycosyl torsion angles are also likely to be similar while the molecules are bound to the enzyme. The MOPAC program has a tendency to flatten five-membered furanose rings into an unfavored, eclipsed configuration, which

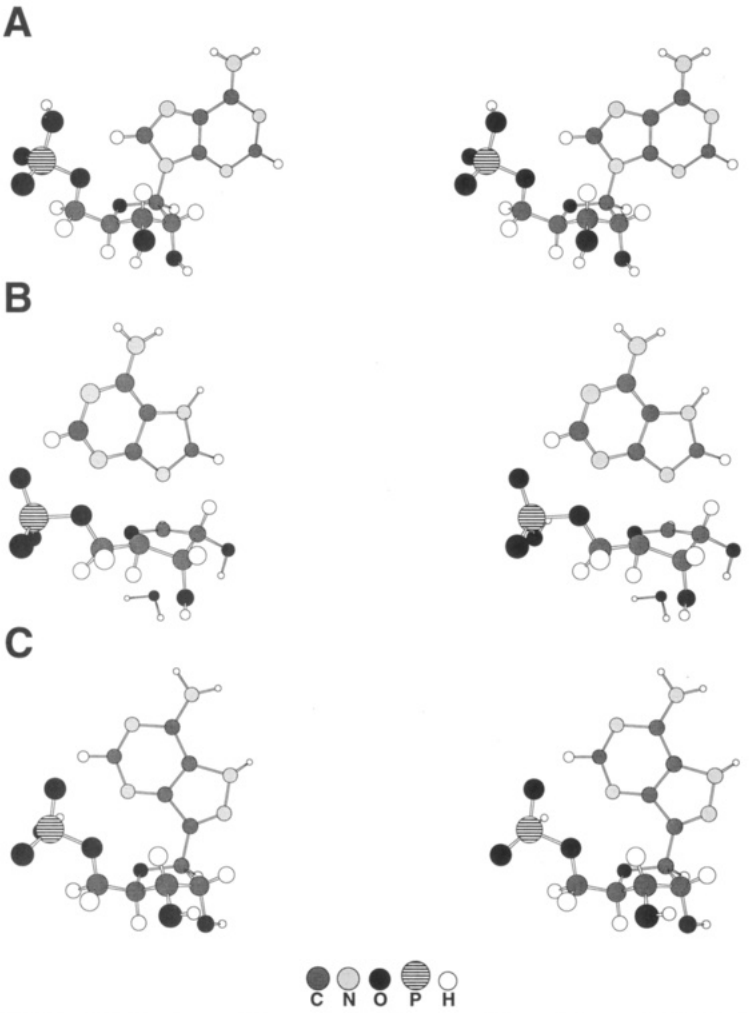

FIGURE 2: Stereoviews of AMP (A), AMP in the transition-state configuration (B), and formycin 5′-PO_4 (C). The conformation of AMP is taken from the crystal structure (Kraut & Jensen, 1963) which is similar to that in solution as determined by NMR analysis [e.g., Sundaralingam (1975)]. The transition-state structure is based on that for AMP nucleosidase in the presence of MgATP (Mentch et al., 1987). Coordinates for formycin 5′-PO_4 (FMP) are from the X-ray crystal structure of Giranda et al. (1988). Hydrogen atoms are positioned by molecular orbital minimization. Features of the transition state include *syn* conformation of adenine with respect to ribose, N7 protonation, bond order of 0.18 for N9–C1′, rehybridization of C1′ to near sp^2 geometry, change in ribose pucker to 3′-exo, and weak participation of the water nucleophile with a bond order of 0.03. Note the *syn* conformation for formycin 5′-PO_4 (C) and protonation of N7.

differs from that known to exist in X-ray crystal and NMR structures (Giranda et al., 1988; Kraut & Jensen, 1963; Sundaralingam, 1975). Furanose rings were fixed with the 3′-endo and 3′-exo configurations known to predominate in substrate and transition-state structures, respectively (Horenstein et al., 1991).

All nucleotide monophosphates were modeled with one phosphate oxygen protonated. The starting structure for AMP in solution was from the X-ray crystal structure coordinates (Kraut & Jensen, 1963). Formycin 5′-PO_4 is a strong ($K_m/K_{is} \geq 1200$) inhibitor of AMP nucleosidase, and it was assumed that the solution configuration of formycin is close to that for enzyme-bound nucleotides (DeWolf et al., 1979). The crystal structure of formycin 5′-PO_4 was used as the structural template for enzyme-bound non-transition-state species. This structure has a favorable, staggered 3′-endo ribose ring, a *syn* configuration for the purine ring (as opposed to AMP, which has an *anti*-glycosyl torsion angle), and an extended phosphoryl arm. Protons not located in the crystal structure were added before calculations. The bond and dihedral angles of the added protons were left unconstrained to minimize the geometry of this structure, as was the phosphate torsion angle. Formycin was N3-protonated in the crystal but is not at physiological pH; therefore, the minimization routine was allowed to rotate the phosphate to form an optimal hydrogen bond between the phosphate proton and N3. All other bond and dihedral angles were fixed. Bond lengths were left unconstrained for calculations on nucleotides.

The starting geometry for AMP in the Michaelis complex was obtained by making appropriate modifications to the minimized formycin 5′-PO_4 structure, based on the evidence that the transition state has a structure similar to that of formycin 5′-PO_4 (Giranda et al., 1988). As with formycin 5′-PO_4, all angles, except for those describing newly added protons or oxygens, were constrained in order to retain the desired configuration.

The BEBOVIB-IV procedure (Sims & Lewis, 1984; Sims et al., 1977) only provides information about the structure of the molecular fragment proximal to the breaking C1′–N9 bond. A full-molecule structure was required for modeling of the complete transition states. The transition-state structure for AMP contained a 3′-exo ribose ring, C1′ fully bonded only to H1′, O4′, and C2′ in a near-planar sp^2 geometry; a C2′–H2′ bond perpendicular to and above the ribose plane to permit hyperconjugation; an extended phosphoryl arm; a *syn*-glycosyl torsion angle which is isosteric with that in the formycin crystal structure; an N7-protonated adenine leaving group orthogonal to the ribose plane; and an optional attacking

Table 1: Molecular Parameters of the Transition State of AMP Nucleosidase in the Presence of ATP

bond	bond length (Å)	bond order	source
C1′–N9	1.960	0.21	*a*
C1′–O4′	1.281	1.73	*a*
C1′–C2′	1.500	1.03	*a*
C1′–H1′	1.100	1.00	*a*
C1′–O (attacking water)	2.497	0.03	*a*
C2′–H2′	1.109	0.97	*a*
C2–N3	1.316		*b*
C2–H2	1.030		*b*
C4′–C3′	1.495		*b*
C5′–C4′	1.521		*b*
C4′–H4′	1.103		*b*
C5′–O5′	1.385		*b*
O5′–P	1.677		*b*
H–O(P)	0.950		*b*
N9–C1′–(H1′,O4′,C2′)	bond angle = 90.663°		*a*

[a] Geometry from BEBOVIB analyses of the transition state (Mentch et al., 1987). [b] Required to be fixed to maintain the integrity of the model, as revealed by preliminary calculations.

nucleophile (H_2O or HO^-) below the plane of the ribose ring and collinear with the breaking C1′–N9 bond (Figure 2). Bond lengths and angles around C1′ were fixed at the appropriate values determined from kinetic isotope effects and BEBOVIB analysis (Table 1). Additional bond lengths were also fixed as indicated in Table 1 to prevent ring opening and inappropriate bond distortions during minimization. The remaining bond lengths were allowed to vary during the molecular orbital calculations, but all bond and dihedral angles were fixed.

RESULTS AND DISCUSSION

Electrostatic Potential Surface of AMP. The molecular electrostatic potential surfaces calculated for the conformation of free and enzyme-bound AMP are shown in panels A and B of Figure 3. The oxygens of the phosphate group have substantial negative charge (blue). Partial negative charges (blue-green) also reside on the lone pairs of oxygens in the ribose ring and of the disubstituted purine nitrogens (N1, N3, and N7). Trisubstituted nitrogens (N6 and N9), all carbons, and alkyl protons distal to the glycosidic bond have intermediate electron density (green). Partial positive charges (orange) are located on alcohol and amide protons, as well as alkyl protons proximal to the glycosidic bond (H8 and H1′). Positively and negatively charged groups may serve as hydrogen bond donors and acceptors, respectively, during binding interactions with the enzyme. When AMP is bound, distortion of the N-glycosidic torsion angle induces strain in the bond and causes electron deficiency to appear in the C1′ proton (black arrows, compare panels A and B of Figure 3). The phosphate proton and N3 of the purine are within hydrogen-bonding distance in this structure. The X-ray crystal structure of formycin 5′-PO_4 also shows a hydrogen bond between N3 and the phosphoryl (Giranda et al., 1989). Distortion of the N-glycosidic bond of AMP in the Michaelis complex is proposed to be an early step in destabilizing the bond.

Electrostatic Potential Surfaces of the Enzyme-Stabilized Transition State. The transition-state structures for native and V_{max} mutant AMP nucleosidases are characterized by C1′–N9 bond orders of 0.21 and 0.18 when determined in the presence of allosteric activator (Mentch et al., 1987; Parkin et al., 1991). Electrostatic potential surfaces were calculated for both structures but gave no apparent difference in surface charge by visual inspection of charge maps similar to those in Figure 3. The changes in the measured V_{max} values for these systems can thus be attributed to the differences in oxycarbonium stabilization at the transition state (Parkin et al., 1991) rather than major differences in molecular electrostatic potentials. This result is consistent with reports that large changes in reactivity result from small changes in reactive group distance and alignment [e.g., Bruice (1976)]. The transition-state molecular electrostatic potential surfaces in Figures 3C and 4 were calculated for the native AMP nucleosidase in the presence of allosteric activator.

One principal difference between enzyme-bound substrate (Figure 3B) and the transition state (Figure 3C) is the accumulation of positive charge on N7 of the transition state, due to its protonation by the enzyme. In contrast, bound substrate has partial negative charge at this position (white arrows, panels B and C of Figure 3). Enzymatic groups which interact with the positively charged N7 would be expected to play a major role in catalysis since protonation of N7 occurs only as the glycosidic bond is sufficiently weakened to cause an increase in the pK_a for N7, followed by protonation from an enzymatic group prior to formation of the transition state (Mentch et al., 1987). Thus a recognition feature of the transition state is the partial positive charge at N7. The presence of the weakly bonded hydroxyl nucleophile is also part of the transition-state ensemble (Figure 3C). Since the bond order to the attacking hydroxyl is low, the hydroxyl is strongly electronegative, which also influences the hydroxyl ion hydrogen to be relatively electron rich, unlike hydrogens of the 2′- and 3′-hydroxyls bound to aliphatic alcohols. Similar results are obtained when H_2O is used as the preassociated nucleophile, although the charge differences are not as great.

Electrostatic Potential Surfaces of the Transition State without the Incipient Nucleophile. Solvolysis of AMP nucleosidase in the presence of methanol demonstrates that the water is a specific nucleophile (DeWolf et al., 1986). The transition-state oxycarbonium is not accessible to bulk solvent; thus the attacking nucleophile is an enzyme-bound H_2O or OH^-. In the absence of an attacking nucleophile (Figure 4), positive charge in excess of that bound to substrate remains on C1′ and H1′ in the transition state (compare Figures 3B and 4). However, when hydroxyl ion is present, the additional negative charge on the attacking oxygen makes H1′ less positive than in bound substrate (black arrow, panels B and C of Figure 3). A transition state without preassociated nucleophile also results in the accumulation of significant positive charge on C1′ (Figure 4, blue arrows) and partial positive charge on O4′ (Figures 4 and 3C, yellow arrows). The positively charged oxycarbonium character in the transition-state without preassociated nucleophile suggests that the enzyme stabilizes the developing transition state chemistry by enforcing participation of the activated nucleophile, which spares the requirement for additional neutralizing groups from the enzyme. The presence of a preassociated nucleophile in solution chemistry is thought to be necessary to allow formation of oxycarbonium-like transition states (Jencks, 1980).

Effect of Hydroxyl Geometry on the Electrostatic Potential Surface of the Transition State. Rotation to place the 2′- and 3′-hydroxyl groups in different configurations has a minimal energy requirement but has been shown to influence the molecular electrostatic potential surface of inosine at the transition state of nucleoside hydrolase (Horenstein & Schramm, 1993a). The oxycarbonium character of the transition state for AMP nucleosidase is modestly influenced by these changes when determined without the preassociated nucleophile (Figure 4, blue and yellow arrows). However,

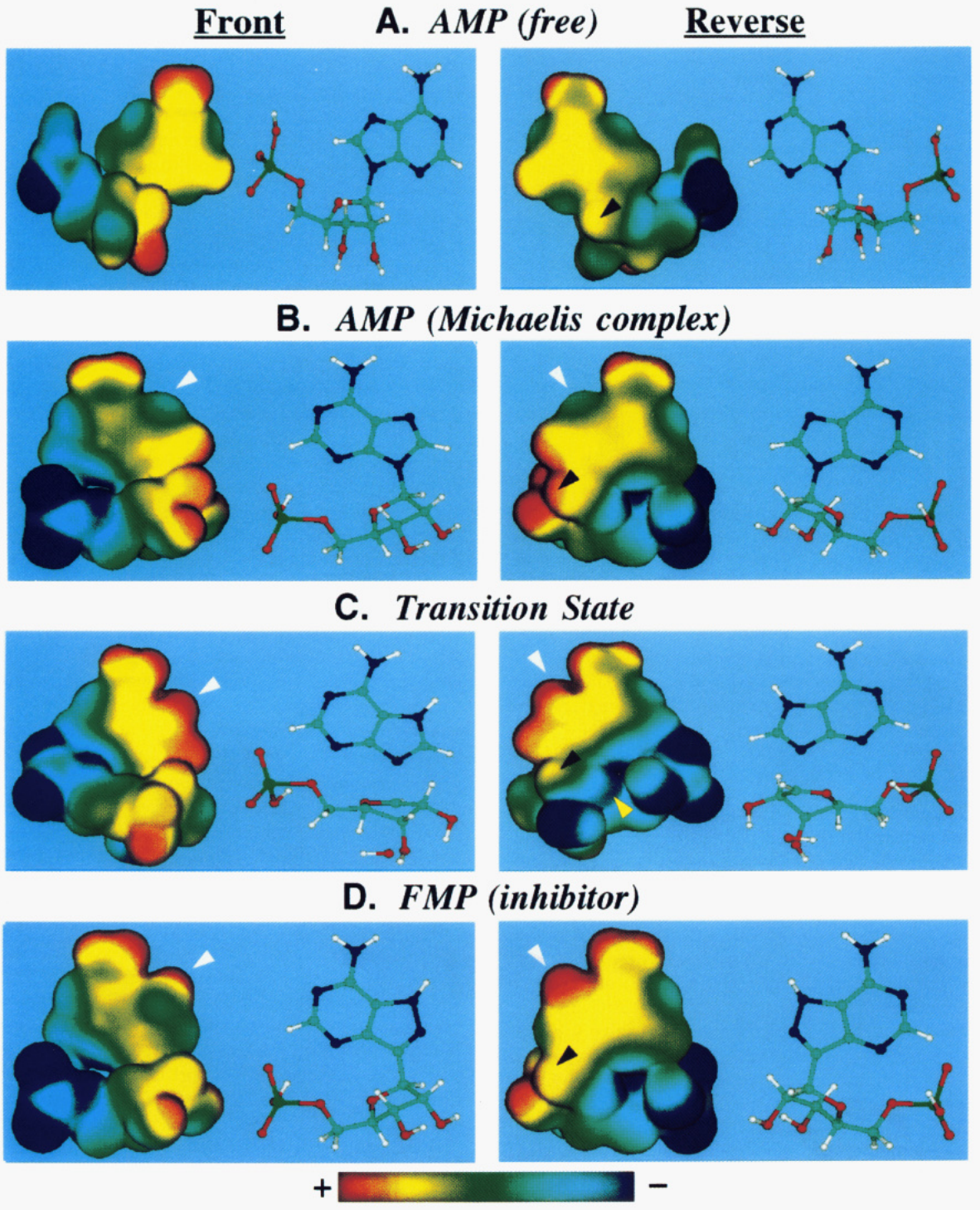

FIGURE 3: Molecular electrostatic potential surfaces for AMP in solution (A), bound to AMP nucleosidase in the Michaelis complex (B), and at the transition state of AMP nucleosidase (C) and for formycin 5′-PO_4 (D). The stick models use the color code white = hydrogen, purple = nitrogen, green = carbon, red = oxygen, and bright green = phosphorus. The stick models are shown in the same orientation as the electrostatic potential surfaces. Left and right panels are 180° horizontal rotations of the same molecule. The color code for electrostatic potential surfaces uses blue and red to indicate the most negative and positive electrostatic potentials, respectively. The energy difference between the most positive and negative regions in the color scale is approximately 63 kcal/mol (electrostatic potential × unit charge). Surface potential is displayed at an electron density of $0.002e/a_0^3$, which is the volume surrounding >95% of the total electron density and is near the van der Waals surface (Sjoberg & Politzar, 1990). The white arrows in panels B–D indicate the N7 position in AMP and the transition state and the corresponding position in formycin 5′-PO_4. Note that this position is protonated and has a positive potential surface (electron deficient) in both the transition state and in formycin 5′-PO_4 but is slightly negative in free and bound AMP. The black arrow shown in the right panels indicates the proton on C1′. For bound AMP (B), glycosidic bond distortion causes substantial electron deficiency at the anomeric proton (black arrows, compare with panel A). In the transition state, participation of the hydroxide nucleophile provides sufficient electron donation to neutralize this site even though the ribosyl group has strongly developed oxycarbonium character. Without the participation of the hydroxyl, this group is strongly positive (compare to the sites indicated by blue arrows in Figure 4). Hydroxide neutralization of transition-state charge is also evident from the charge at O4′ in the transition state by comparing the net negative charge in the transition state with the neutral charge in the absence of hydroxide (compare yellow arrows in panel C and Figure 4). For the electrostatic surfaces in this figure, the ribose conformation is 3′-endo for AMP and formycin 5′-PO_4 and is 3′-exo in the transition state as a consequence of rehybridization of C1′ to sp^2. Since the energy barrier for 3′-endo to 3′-exo is modest, it is anticipated that the enzyme would enforce the 3′-exo configuration when binding formycin 5′-PO_4 as a transition-state analogue.

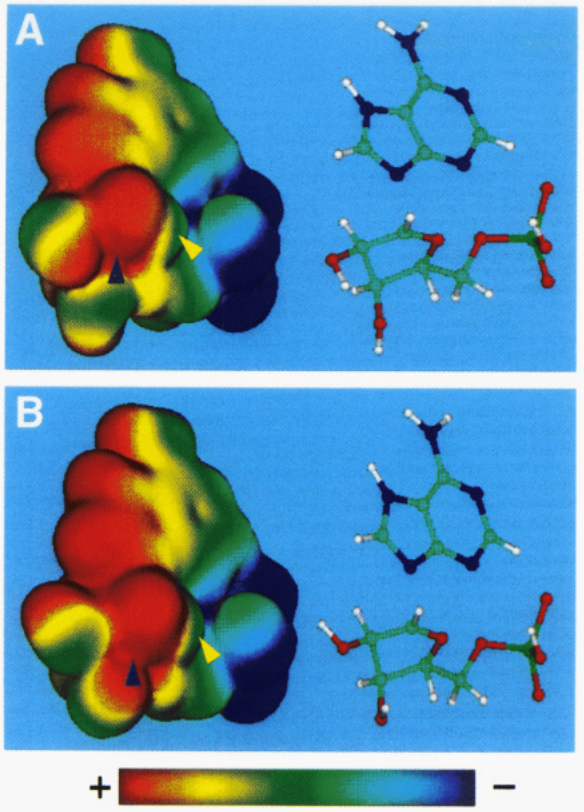

FIGURE 4: Electrostatic potential surface of AMP at the transition state imposed by AMP nucleosidase. The water/hydroxyl nucleophile has been omitted from the calculations. The molecules are tilted to expose the lower surface of the ribose where oxycarbonium ion formation is most apparent. The yellow arrows indicate the O4′ ribosyl atom while the blue arrows indicate the location of C1′. The rotomeric conformation of the hydroxyls at the 2′- and 3′-carbons was altered to illustrate the changes in electrostatic distribution near C1′ which occur with altered hydroxyl conformation. The color codes for atoms and charge are the same as in Figure 3.

the positive charge on H8 can be stabilized by O2′ when in the conformation of Figure 4A. The overall similarities of the molecular electrostatic potentials suggest that the hydroxyl rotomers can assume a variety of conformations to optimize the low-barrier reaction path to the transition state. The actual rotomeric conformation will be a function of the geometry of the nucleophile as presented by the enzyme and hydrogen-bonding interactions which are involved in substrate binding and transition-state stabilization. The protein structure with a bound transition-state analogue will be required to resolve this geometry.

Electrostatic Potential Surface of Formycin 5′-PO_4. The tight-binding inhibitor formycin 5′-PO_4 has a nitrogen and carbon transposed in the five-membered ring of the purine (Figure 1). The C7–C1′ glycosidic bond is stable to hydrolysis, and the N7 isosteric with the N7 of AMP is protonated at neutral pH to maintain the planar geometry. The solution structures of AMP (Figure 3A) and formycin 5′-PO_4 (Figure 3D) differ considerably, both in their molecular electrostatic potential surfaces and in their geometry. Differences in electrostatics exist at N7 (Figure 3D, white arrow), which like the transition state but unlike the substrate is positively charged; position 8, which in formycin is negatively charged (this position has partial positive charge in the Michaelis complex and transition state); and H1′, which is less positively charged than in AMP and comparable in charge to the transition state (Figure 3D, black arrow). The solution structure of formycin 5′-PO_4 more closely resembles the transition state than does the substrate (compare panels A, C, and D of Figure 3), and is inert to the enzymatic reaction; its characteristic as an inhibitor can be easily understood from both the conformational and electrostatic similarity to the enzyme-stabilized transition state. The visual match between inhibitor and transition state (panels C and D of Figure 3) provides qualitative support for formycin 5′-PO_4 as a transition-state analogue. Quantitative analysis by a complementarity index which includes both geometric and molecular electrostatic potential surface information would be even more helpful. No such algorithm is currently available although research has been progressing in this area using atomic partial charges and atomic volumes (Kearsley & Smith, 1992).

CONCLUSIONS

The molecular electrostatic potential surfaces of AMP, FMP, and the transition state of the AMP nucleosidase reaction provide insights into the mechanism which the enzyme might use to achieve catalysis by stabilizing the transition state. The charge and geometry of the purine base, ribose, and phosphoryl group in the transition state are similar to those in the ground-state structure of formycin 5′-PO_4. Both the transition state and the crystal structure of formycin 5′-PO_4 appear to be stabilized by an internal hydrogen bond between N3 of the purine and the phosphoryl (Giranda et al., 1988). Analysis of the transition-state charges reveals a partial oxocarbonium character consistent with the expanded-S_N2 mechanism predicted from kinetic isotope effects. The molecular electrostatic potentials suggest that the attacking hydroxyl ion nucleophile plays a major role in the stabilization of the oxocarbonium. An enzymatic base which binds water and abstracts a proton could be envisioned to contribute to catalysis by (a) bringing water into proximity with the enzymatically bound and destabilized AMP in the correct orientation, (b) activating the reactant, and (c) neutralizing the developing positive charge of the oxycarbonium.

Transition-state molecular electrostatic potential analysis defines the features which characterize a compound as a transition-state inhibitor. The natural product formycin 5′-PO_4 mimics several unique charge features of the transition state. It has a partial positive charge on N7 due to stable protonation at that position and the internal hydrogen bond which stabilizes the *syn*-glycosyl torsion angle. Distortion of AMP to the *syn* torsion angle destabilizes the glycosidic bond and thus characterizes a feature of the transition-state binding. The hydrolytically stable carbon–carbon glycosidic bond lacks the electron-withdrawing character of the carbon–nitrogen bond of the substrate, causing H1′ to resemble the charge located in that position of the transition state. The molecular electrostatic potentials shown in Figure 3 provide a clear explanation for the inhibition of AMP nucleosidase by formycin 5′-PO_4. Transition-state charge and geometry can be a valuable guide for the synthesis of transition-state inhibitors and the interpretation of their action.

REFERENCES

Boutellier, M., Horenstein, B. A., Semenyaka, A., Schramm, V. L., & Ganem, B. (1994) *Biochemistry 33*, 3994–4000.
Bruice, T. C. (1976) *Annu. Rev. Biochem. 45*, 331–373.
DeWolf, W. E., Jr., Fullin, F. A., & Schramm, V. L. (1979) *J. Biol. Chem. 254*, 10868–10875.
DeWolf, W. E., Jr., Emig, F. A., & Schramm, V. L. (1986) *Biochemistry 25*, 4132–4140.
Frisch, M. J., Trucks, G. W., Hend-Gordon, M., Gill, P. M. W., Wong, M. W., Foresman, J. B., Johnson, B. G., Schlegel, H. B., Robb, M. A., Replogle, E. S., Gomperts, R., Andres, J. L., Raghavachari, K., Binkley, J. S., Gonzalez, C., Martin, R. L.,

Fox, D. J., DeFrees, D. J., Baker, J., Stewart, J. J. P., & Pople, J. A. (1992) *Gaussian 92 user's guide*, Gaussian Inc., Pittsburgh, PA.
Giranda, V. L., Berman, H. M., & Schramm, V. L. (1988) *Biochemistry 27*, 5813–5818.
Gouverneur, V. E., Houk, K. N., de Pascual-Teresa, B., Beno, B., Janda, K. D., & Lerner, R. (1993) *Science 262*, 204–208.
Horenstein, B. A., & Schramm, V. L. (1993a) *Biochemistry 32*, 7089–7097.
Horenstein, B. A., & Schramm, V. L. (1993b) *Biochemistry 32*, 9917–9925.
Horenstein, B. A., Parkin, D. W., Estupinan, B., & Schramm, V. L. (1991) *Biochemistry 30*, 10788–10795.
Jencks, W. P. (1980) *Acc. Chem. Res. 13*, 161–169.
Kearsley, S. K., & Smith, G. M. (1992) *Tetrahedron Comput. Methodol. 3*, 615–633.
Kline, P. C., & Schramm, V. L. (1994) (submitted for publication).
Kraut, J., & Jensen, L. H. (1963) *Acta Crystallogr. 16*, 79–88.
Markham, G. D., Parkin, D. W., Mentch, F., & Schramm, V. L. (1987) *J. Biol. Chem. 262*, 5609–5615.
Mentch, F., Parkin, D. W., & Schramm, V. L. (1987) *Biochemistry 26*, 921–930.
Merz, K. M., Jr., & Besler, B. H. (1990) *Quantum Chemistry Program Exchange*, No. 589, Indiana University, Bloomington, IN.
Parkin, D. W., & Schramm, V. L. (1984) *J. Biol. Chem. 259*, 9418–9425.
Parkin, D. W., & Schramm, V. L. (1987) *Biochemistry 26*, 913–920.
Parkin, D. W., Leung, H. B., & Schramm, V. L. (1984) *J. Biol. Chem. 259*, 9411–9417.
Parkin, D. W., Mentch, F., Banks, G. A., Horenstein, B. A., & Schramm, V. L. (1991) *Biochemistry 30*, 921–930.
Schramm, V. L. (1974) *J. Biol. Chem. 249*, 1729–1736.
Schramm, V. L., & Leung, H. B. (1973) *J. Biol. Chem. 248*, 8313–8315.
Sims, L. B., & Lewis, D. E. (1984) in *Isotopes in Organic Chemistry* (Buncel, E., & Lee, C. C., Eds.) Vol. 6, pp 161–259, Elsevier, New York.
Sims, L. B., Burton, G. W., & Lewis, D. E. (1977) *BEBOVIB-IV, Quantum Chemistry Program Exchange*, No. 337, Indiana University, Bloomington, IN.
Sjoberg, P., & Politzer, P. (1990) *J. Phys. Chem. 94*, 3959–3961.
Suhadolnik, R. J. (1979) in *Nucleosides as Biological Probes*, pp 169–183, John Wiley & Sons, New York.
Sundaralingam, M. (1975) in *Structure and Conformation of Nucleic Acids and Protein–Nucleic Acid Interactions* (Sundaralingam, M., & Rao, S. T., Eds.) pp 487–524, University Park Press, Baltimore, MD.
Warshel, A. (1991) *Computer Modeling of Chemical Reactions in Enzymes and Solutions*, Chapter 9, John Wiley & Sons, New York.
Warshel, A., Naray-Szabo, G., Sussman, F., & Hwang, J.-K. (1989) *Biochemistry 28*, 3629–3637.
Wolfenden, R. (1972) *Acc. Chem. Res. 5*, 10–18.